Tomographic Imaging of Molecular Orbitals in Length and Velocity Form

Elmar V. van der Zwan and Manfred Lein

Institute for Physics, University of Kassel, Heinrich-Plett-Strasse 40, 34132 Kassel,Germany

Abstract. Recently Itatani *et al.* [Nature **432**, 876 (2004)] introduced the new concept of molecular orbital tomography, where high harmonic generation (HHG) is used to image electronic wave functions. We describe an alternative reconstruction form, using momentum instead of dipole matrix elements for the electron recombination step in HHG. We show that using this *velocity-form reconstruction*, one obtains better results than using the original *length-form reconstruction*. We provide numerical evidence for our claim that one has to resort to extremely short pulses to perform the reconstruction for an orbital with arbitrary symmetry. The numerical evidence is based on the exact solution of the time-dependent Schrödinger equation for 2D model systems to simulate the experiment. Furthermore we show that in the case of cylindrically symmetric orbitals, such as the N_2 orbital that was reconstructed in the original work, one can obtain the full 3D wave function and not only a 2D projection of it.

Keywords: molecular orbital tomography, high harmonic generation, error reduction, femtosecond pulses
PACS: 33.80.Rv, 42.65.Ky

INTRODUCTION

In molecules subject to strong laser fields, the non-linear process of high harmonic generation (HHG) takes place. In this process, many laser photons are converted into a single high-frequency photon. In the three-step picture [1], it is explained as a sequence of field ionization, acceleration of the free electron in the laser field, and recollision with the core. The high harmonics have been used for a wide range of applications, ranging from the generation of attosecond pulse trains [2, 3, 4] and single attosecond bursts [5, 6], to the determination of internuclear distances [7, 8]. A new application is the imaging of electronic orbitals using high harmonics in a scheme known as molecular orbital tomography [9]. By approximating the returning electron in the three-step model as a plane wave, the matrix element describing the recombination becomes a Fourier transform. For N_2, harmonic spectra for many different alignment angles of the molecules in the laser field were combined to reconstruct the electronic orbital, i.e. the values of the wave function, not only the modulus squared. For this reconstruction, information about the continuum wave packet at the moment of return to the ion is needed. This information is taken from an atomic reference system that has the same ionization potential as the system of interest. The idea is that for such a system, the tunneling and propagation steps of the three-step model for HHG are similar to those of the molecule. Having knowledge about the electronic orbital of the reference system and its harmonics, this leads to knowledge about the continuum wave packet and thus allows the reconstruction of the molecular orbital.

It was recently shown for various rare-gas atoms that indeed the continuum wave packet has very similar structure independent of the species [10]. Also for more complex molecules the orientation dependence of HHG can still be understood in a single-active electron approximation [11]. Both observations support the idea of extending the technique to more complex systems. It has been argued that tomography becomes more reliable if one moves to longer wavelengths [12]. For the quantitative analysis of the results, one should take multi-electron effects into account, as more than one electron contributes to the high harmonics [13]. As a consequence, a modified Dyson orbital and not the highest occupied molecular orbital is reconstructed [14, 15].

In the original work the reconstruction was based on dipole matrix elements. It has been recently reported that the use of momentum matrix elements leads to more accurate results for molecular HHG [16], which suggests that momentum matrix elements should be used in molecular tomography. Elsewhere we show that formally the reconstruction is only possible in two cases; either (i) if the orbital is *(un-)gerade* or (ii) if the wave packets approach the core always from the same side. The latter can be achieved e.g. using extremely short pulses, and a suitable pulse is proposed in [17]. Here we provide numerical evidence for both claims, i.e. that the orbital is more accurately reconstructed using momentum matrix elements, and that reconstruction of an asymmetric orbital is impossible using many-cycle pulses. Furthermore,

we give an intuitive derivation of the last statement.

MOLECULAR ORBITAL TOMOGRAPHY

To understand the principles of the tomographic reconstruction, we consider a diatomic molecular system in a laser field polarized in the x-direction and propagating in the z-direction. The orientation of the molecule is given by two angles (ϕ, ϑ). Here, $\phi \in [0, \pi]$ denotes the orientation relative to the z-axis, while $\vartheta \in [0, 2\pi]$ describes the rotation around the z-axis. The harmonics for a molecule with orientation (ϕ, ϑ) are then characterized by

$$I_{\phi,\vartheta}(\omega) = \omega^4(|\mathbf{D}_{\phi,\vartheta}(\omega)|^2 + |\mathbf{D}_{\phi,\vartheta}(-\omega)|^2), \tag{1a}$$

$$\Phi_{\phi,\vartheta}(\omega) = \arg[\mathbf{D}_{\phi,\vartheta}(\omega)], \tag{1b}$$

where $I_{\phi,\vartheta}(\omega)$ is the intensity in arbitrary units and $\Phi_{\phi,\vartheta}(\omega)$ the phase of a harmonic with frequency ω. If we assume one active electron, the Fourier transformed dipole moment $\mathbf{D}(\omega)$ is given by (for simplicity we drop the angle dependence)

$$\mathbf{D}(\omega) = \int \langle \mathbf{d}(t) \rangle e^{i\omega t} dt, \tag{2a}$$

$$\langle \mathbf{d}(t) \rangle = \langle \psi(x,y,z,t) | -\mathbf{r} | \psi(x,y,z,t) \rangle, \tag{2b}$$

where $\mathbf{r} = \binom{x}{y}$. Here and in the following, we use atomic units. We therefore have $I(\omega) = 2\omega^4 |\mathbf{D}(\omega)|^2$. We split the time-dependent wave function ψ in two parts as $\psi(x,y,z,t) = \psi_0(x,y,z,t) + \psi_c(x,y,z,t)$, where $\psi_0(x,y,z,t)$ is the initial bound-state wave function and $\psi_c(x,y,z,t)$ is the continuum wave packet. The time-dependence of the initial state is given by

$$\psi_0(x,y,z,t) = \psi_0(x,y,z)e^{iI_p t}, \tag{3}$$

where $\psi_0(x,y,z)$ is the time-independent initial state of the electron (chosen to be real) and $-I_p$ is its energy. Introducing the plane-wave approximation, a downward moving continuum wave packet (i.e. returning to the core from $x > 0$) can be written as

$$\psi_c(x,y,z,t) = \int_{-\infty}^{\infty} a(k)e^{-ikx}e^{-i\frac{k^2}{2}t} \frac{dk}{2\pi}, \tag{4}$$

where the $a(k)$ are complex amplitudes. Neglecting depletion of the initial state and assuming that all momentum components have negative momentum (i.e. $k > 0$ in our notation), this leads to

$$\mathbf{D}(\omega) = \frac{a[k(\omega)]}{k(\omega)} \iint \left[\int \psi_0(x,y,z)dz \right] (-\mathbf{r})e^{-ik(\omega)x} d^2\mathbf{r}, \tag{5}$$

with $k(\omega) = \sqrt{2(\omega - I_p)}$. In practice, the wave number $k(\omega) = \sqrt{2(\omega)}$ is used [9], as supported by numerical tests that we have performed. The physical argument is that, when describing the returning electron as a plane wave, we should take into account that at the moment of recombination its wave number is modified by the absorption of I_p into the kinetic energy. However, for calculations of the spectra based on the strong-field approximation (SFA) it was recently reported that the energy-conserving relation $k(\omega) = \sqrt{2(\omega - I_p)}$ should be used [12]. It should be noted that in [9] only the harmonic intensities were measured, although it is now in principle possible to measure also the harmonic phases [18, 19, 20, 21]. In our simulations we record the phases numerically and use them for the reconstructions.

Note that since in reality $a[k(\omega)]$ depends on time, equation (4) is not a rigorous equation, but gives an intuitive interpretation of $a[k(\omega)]$. The precise definition of $a[k(\omega)]$ is provided by equation (5). There are two unknowns in equation (5), namely $a[k(\omega)]$ and $\psi_0(x,y,z)$. One of the main ideas of the procedure is to solve this problem by looking at an (atomic) reference system for which $\psi_0^{(a)}(x,y,z)$ is known and $a^{(a)}[k(\omega)]$ is very similar to $a[k(\omega)]$, where with a superscript '(a)' we denote reference system quantities. This is approximately the case if the reference system and the molecule of interest have the same ionization potential [9]. However, problems arise in the multi-photon regime [22, 23]. Therefore the system should be preferably such that the Keldysh parameter $K = \omega_L \sqrt{2I_p}/E_0$ is significantly lower as 1, but not too low as that introduces depletion. Here ω_L is the fundamental laser frequency and E_0 is the maximum of the laser electric field.

571

In the experimental implementation [9], the molecules are aligned along directions within the xy-plane, so that the angle ϑ becomes equal to the angle θ between the molecular axis and the electric field. Harmonic generation is then considered for all orientations θ and is determined by the rotated projection on the xy-plane of the bound state,

$$\psi_{0,\theta}^{2D}(x,y) = \int \psi_0(x\cos\theta + y\sin\theta, -x\sin\theta + y\cos\theta, z)dz, \tag{6}$$

through the Fourier elements

$$\mathbf{d}_{\frac{\pi}{2},\theta}(\omega) \equiv \iint \psi_{0,\theta}^{2D}(x,y)\mathbf{r}e^{-ik(\omega)x}d^2\mathbf{r} \tag{7}$$

in equation (5). Using the Fourier slice theorem, these transforms can be inverted to obtain

$$\psi_0^{2D}(x,y) = \frac{1}{2(2\pi)^2}\left\{\frac{1}{x}\iint (d_{\theta,x}(\omega)\cos\theta + d_{\theta,y}(\omega)\sin\theta) \times e^{ik(\omega)(x\cos\theta - y\sin\theta)}d\omega d\theta\right.$$

$$\left. + \frac{1}{y}\iint (-d_{\theta,x}(\omega)\sin\theta + d_{\theta,y}(\omega)\cos\theta) \times e^{ik(\omega)(x\cos\theta - y\sin\theta)}d\omega d\theta\right\}. \tag{8}$$

LENGTH VERSUS VELOCITY FORM

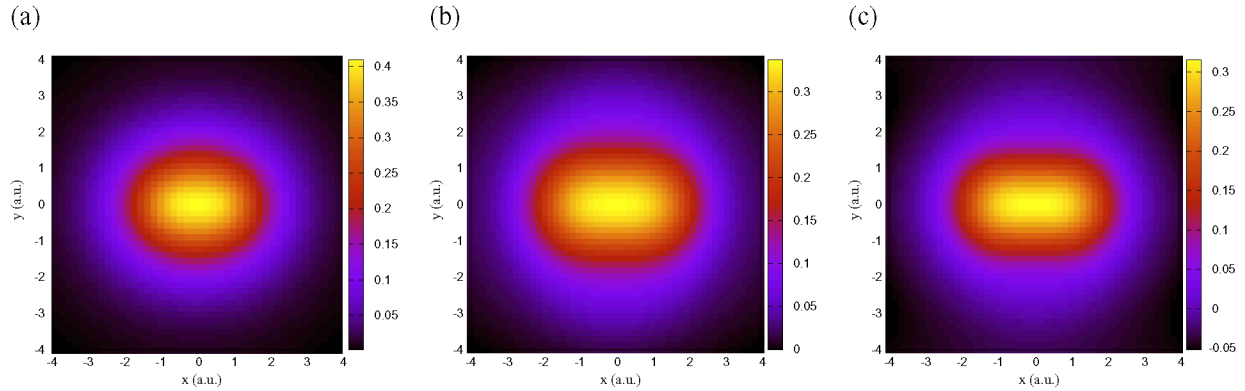(a)　　　　　　　　　(b)　　　　　　　　　(c)

FIGURE 1. Results of the simulation. (a) the 2D H_2^+ ground-state wave function, (b) the result obtained with length-form reconstruction, (c) the result obtained with velocity-form reconstruction. All orbitals plotted as functions of x,y in atomic units.

As introduced in [17], the reconstruction can also be performed using momentum matrix elements. We call this approach the *velocity-form reconstruction*. Using the Ehrenfest theorem, the harmonics can be equivalenty described by

$$I(\omega) = 2\omega^2 |P_x(\omega)|^2, \tag{9a}$$

$$P_x(\omega) = -a[k(\omega)]\, p(\omega), \tag{9b}$$

$$p(\omega) = \iint \psi_0^{2D}(x,y)e^{-ik(\omega)x}d^2\mathbf{r}. \tag{9c}$$

The reconstruction equation then takes the form

$$\psi_0^{2D}(x,y) = \frac{1}{(2\pi)^2}\iint p_\theta(\omega)e^{ik(\omega)(x\cos\theta - y\sin\theta)}d\omega d\theta. \tag{10}$$

We present here simulations of the tomography experiment for the ground state of a 2D model of H_2^+. The simulations consist of several steps. First we solve the time-dependent Schrödinger equation (TDSE) numerically using the split-operator method [24] for both the molecule of interest and the reference system. Then the HHG spectra are calculated from the acceleration expectation value [25]. The model molecule has an internuclear distance of $R = 2.0$ au and is characterized by the softcore potential

$$V(\mathbf{r}) = -\frac{1}{\sqrt{(\mathbf{r} + \frac{\mathbf{R}}{2})^2 + a^2}} - \frac{1}{\sqrt{(\mathbf{r} - \frac{\mathbf{R}}{2})^2 + a^2}}, \tag{11}$$

572

where the softness parameter $a^2 = 0.5$ yields the ionization potential $I_p = 30.2$ eV. We use an intensity of $I = 5 \cdot 10^{14}$ W/cm^2 and a laser wavelength $\lambda = 780$ nm for the applied 3-cycle cos^2-pulse, see the discussion below. As a reference system we use 2D atomic He, in the single-active-electron approximation and with a softcore potential with $a^2 = 0.921$, such that the I_p of the reference system is equal to that of the molecular system.

For the case of length-form reconstruction, $a_\theta[k(\omega)]$ is calculated according to

$$a_\theta[k(\omega)] = \frac{-k(\omega)D_x^{(a)}(\omega)}{d_x^{(a)}(\omega)} \sqrt{\frac{P_I(\theta)}{P_I^{(a)}}}, \qquad (12)$$

where $P_I^{(a)}$ is the total ionization yield of the reference system and $P_I(\theta)$ is the same yield for different orientations of the system of interest. Alternatively, for the reconstruction in velocity-form, $a_\theta[k(\omega)]$ is calculated according to

$$a_\theta[k(\omega)] = \frac{-P_x^{(a)}(\omega)}{p^{(a)}(\omega)} \sqrt{\frac{P_I(\theta)}{P_I^{(a)}}}. \qquad (13)$$

The reconstruction matrix elements are obtained from equation (5) or (9b) and the reconstruction is performed according to equation (8) or (10), for reconstruction in length- or velocity-form, respectively. From the results shown in Fig. 1, it is clear that the velocity form reconstructs the orbital more accurately, as the length form overestimates the size of the orbital. This is related to the effect that in H$_2^+$, the two-center interference is not accurately described in the length form [7, 16].

LONG VERSUS SHORT PULSE

(a)   (b)   (c)
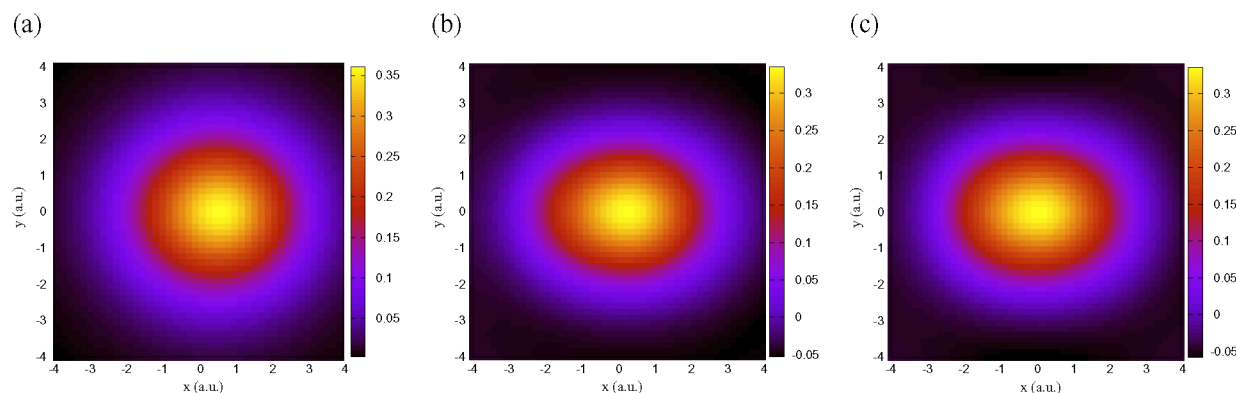

FIGURE 2. Results of the simulation for an asymmetric state. (a) the (H-He)$^{2+}$ ground-state wave function, (b) the result obtained using a 3-cycle pulse and velocity-form reconstruction, (c) the result obtained with a 10-cycle pulse and velocity-form reconstruction. All orbitals plotted as functions of x,y in atomic units.

As mentioned earlier, the reconstruction equations (8) and (10) can formally only be derived for general orbitals in the case we use a short pulse, such that the continuum wave packets aproach the nucleus from only one side. In [17] we show that a good pulse is a 3-cycle cos^2-pulse with a carrier-envelope phase of 0.25π. This is the pulse that was used for the results presented in the previous section. Here we will give numerical evidence that the reconstruction of an asymmetric orbital is not possible using a longer pulse. For this purpose we show the results of simulations for 2D (H-He)$^{2+}$ with fixed internuclear distance $R = 2.2$ au. We use a softcore potential with softness parameter $a^2 = 2.72$ to give the state an ionization potential of $I_p = 30.2$ eV. As an example of a longer pulse, we use a 10-cycle cos^2-pulse with a zero carrier-envelope phase. For the reconstruction using the short pulse, all frequencies of the harmonic spectra contain information and we use all numerical data points for the reconstruction. For the longer pulse, only the odd harmonics are used. In both cases, we use velocity-form reconstruction. From the results in Fig. 2 it is apparent that we need to resort to extremely short pulses in order to perform the reconstruction of an asymmetric state: the long pulse leads inevitably to a symmetric orbital. Other methods to ensure that the wave packets approach the nuclei from one side only are conceivable. A possibility is using the ellipticity of the laser pulse, similar to the polarization gating method in attosecond pulse production [26, 27].

FULL 3D ORBITAL

In a real experiment, the whole orbital -and not just a slice through it at $z = 0$- contributes to the recorded high harmonics. Therefore, using molecular orbital tomography, a 2D projection of the orbital, $\psi_0^{2D}(x,y)$, and not the full orbital itself, $\psi_0(x,y,z)$, is reconstructed as we have shown above. We report here that for a system with cylindrical symmetry around the internuclear x-axis, it is possible to convert the projected wave function into the full wave function. That means that for many simple diatomic molecules such as N_2 (the molecule for which the technique was introduced in [9]) the full orbital can be reconstructed.

Consider an orbital $\psi_0^{2D}(x,y)$ that is entirely contained in an area $L_x \times L_y$. Then we can write

$$\psi_0^{2D}(x,y) = \int_{-\infty}^{\infty} \psi_0(x,y,z)dz = 2\int_0^{\frac{L_y}{2}} \psi_0(x,\sqrt{y^2+z^2},0)dz = 2\int_y^{\frac{L_y}{2}} \frac{z'}{\sqrt{z'^2-y^2}}\psi_0(x,z',0)dz', \tag{14}$$

where the first equality comes from the symmetry. We subtract the singluarity at the lower integration boundary and evaluate it analytically, to arrive at

$$\psi_0^{2D}(x,y) = 2\int_y^{\frac{L_y}{2}} \frac{z'}{\sqrt{z'^2-y^2}}\left[\psi_0(x,z',0) - \psi_0(x,y,0)\right]dz' + 2\sqrt{(\frac{L_y}{2})^2 - y^2}\,\psi_0(x,y,0). \tag{15}$$

This is a Volterra equation of the first kind. To invert it numerically we start at the upper integration boundary and work down. This shows that for cylindrically symmetric molecules it is possible to retrieve the full orbital using molecular orbital tomography.

CONCLUSIONS

We have carried out numerical simulations of the tomographic imaging scheme using exact solutions of the TDSE for model systems. We have shown that at least for 2D H_2^+ the reconstruction of the molecular orbital is more accurate using velocity-form reconstruction based on momentum matrix elements, than with length-form reconstruction based on dipole matrix elements. The effect that the length-form description of high harmonic generation yields the wrong two-center interference pattern, works its way through to molecular orbital tomography, which is based on HHG. This results in blown up orbitals when the reconstruction is performed in length form. We have presented numerical evidence for our claim that the reconstruction of an orbital with some asymmetry is only possible if the wave packets return to the core from only one direction. Our method to ensure this is based on using an extremely short, few-cycle only, laser pulse. We have shown that the full orbital of molecules with cylindrical symmetry around their internuclear axis can be reconstructed, although the tomographic reconstruction alone yields only the projection onto the plane orthogonal to the pulse propagation direction. These observations are a step towards applying molecular orbital tomography to image orbitals on a femto-second timescale in dynamical systems.

ACKNOWLEDGMENTS

REFERENCES

1. P. B. Corkum, *Phys. Rev. Lett.* **71**, 1994 (1993).
2. P. M. Paul, E. S. Toma, P. Breger, G. Mullot, F. Augé, P. Balcou, H. G. Muller, and P. Agostini, *Science* **292**, 1689 (2001).
3. Y. Mairesse, A. de Bohan, L. J. Frasinski, H. Merdji, L. C. Dinu, P. Monchicourt, P. Breger, M. Kovačev, R. Taïeb, B. Carré, H. G. Muller, P. Agostini, and P. Salières, *Science* **302**, 1540 (2003).
4. P. Tzallas, D. Charalambidis, N. A. Papadogiannis, K. Witte, and G. D. Tsakiris, *Nature* **426**, 267 (2003).
5. M. Hentschel, R. Kienberger, C. Spielmann, G. A. Reider, N. Milosevic, T. Brabec, P. B. Corkum, U. Heinzmann, M. Drescher, and F. Krausz, *Nature* **414**, 509 (2001).

6. M. Drescher, M. Hentschel, R. Kienberger, G. Tempea, C. Spielmann, G. A. Reider, P. B. Corkum, and F. Krausz, *Science* **291**, 1923 (2001).
7. M. Lein, N. Hay, R. Velotta, J. P. Marangos, and P. L. Knight, *Phys. Rev. A* **66**, 023805 (2002).
8. T. Kanai, S. Minemoto, and H. Sakai, *Nature* **435**, 470 (2005).
9. J. Itatani, J. Levesque, D. Zeidler, H. Niikura, H. Pépin, J. Kieffer, P. B. Corkum, and D. M. Villeneuve, *Nature* **432**, 867 (2004).
10. J. Levesque, D. Zeidler, J. P. Marangos, P. B. Corkum, and D. M. Villeneuve, *Phys. Rev. Lett.* **98**, 183903 (2007).
11. R. Torres, N. Kajumba, J. G. Underwood, J. S. Robinson, S. Baker, J. W. G. Tisch, R. de Nalda, W. A. Bryan, R. Velotta, C. Altucci, I. C. E. Turcu, and J. P. Marangos, *Phys. Rev. Lett.* **98**, 203007 (2007).
12. V.-H. Le, A.-T. Le, R.-H. Xie, and C. D. Lin, *Preprint* (2007), arXiv:physics/0701250v1 [physics.atom-ph].
13. A. Gordon, F. X. Kärtner, N. Rohringer, and R. Santra, *Phys. Rev. Lett.* **96**, 223902 (2006).
14. R. Santra, and A. Gordon, *Phys. Rev. Lett.* **96**, 073906 (2006).
15. S. Patchkovskii, Z. Zhao, T. Brabec, and D. M. Villeneuve, *Phys. Rev. Lett.* **97**, 123003 (2006).
16. C. C. Chirilă, and M. Lein, *Journal of Modern Optics* **54**, 1039 (2007).
17. E. V. van der Zwan, C. C. Chirilă, and M. Lein, *to be published* (2007).
18. T. Sekikawa, T. Kanai, and S. Watanabe, *Phys. Rev. Lett.* **91**, 103902 (2003).
19. K. Varjú, Y. Mairesse, P. Agostini, P. Breger, B. Carré, L. J. Frasinski, E. Gustafsson, P. Johnsson, J. Mauritsson, H. Merdji, P. Monchicourt, A. L'Huillier, and P. Salières, *Phys. Rev. Lett.* **95**, 243901 (2005).
20. Y. Mairesse, and F. Quéré, *Phys. Rev. A* **71**, 011401(R) (2005).
21. T. Kanai, E. J. Takahashi, Y. Nabekawa, and K. Midorikawa, *Phys. Rev. Lett.* **98**, 153904 (2007).
22. S. L. Chin, and P. A. Golovinski, *J. Phys. B* **28**, 55 (1995).
23. Y. Liang, S. Augst, S. L. Chin, Y. Beaudoin, and M. Chaker, *J. Phys. B* **27**, 5119 (1994).
24. M. D. Feit, J. A. Fleck, Jr, and A. Steiger, *J. Comp. Phys.* **47**, 412 (1982).
25. K. Burnett, V. C. Reed, J. Cooper, and P. L. Knight, *Phys. Rev. A* **45**, 3347 (1992).
26. P. B. Corkum, N. H. Burnett, and M. Y. Ivanov, *Opt. Lett.* **19**, 1870 (1994).
27. I. J. Sola, E. Mével, L. Elouga, E. Constant, V. Strelkov, L. Poletto, P. Villoresi, E. Bendetti, J.-P. Caumes, S. Stagira, C. Vozzi, G. Sansone, and M. Nisoli, *Nature Physics* **2**, 319 (2006).